PROCEEDINGS OF SCIENCE

# Amplitude Analyses on Charm Decays at the LHCb Experiment

**Fernanda Gonçalves Abrantes** *[a]

[a] *University of Oxford, United Kingdom*

*E-mail:* fernanda.goncalves.abrantes@cern.ch

Non-leptonic decays of heavy hadrons, such as $B$ and $D$ mesons, have proven to be a rich environment for the study of light meson spectroscopy and also charge-parity violation. For decays of charm hadrons, many problems related to non-perturbative effects arise in the study of strong interactions. Therefore, the usage of hadronic decays to study weak interactions turns out to be a great opportunity to study the dynamics of hadronic interactions and CP violation in these processes via a full amplitude analysis of the corresponding Dalitz Plot. Among the latest LHCb charm amplitude analysis results, the decays $D^+_{(s)} \to \pi^-\pi^+\pi^+$ with a particular emphasis on the measurement of the $\pi^-\pi^+$ S-wave amplitude are presented.

*41st International Conference on High Energy physics - ICHEP2022*
*6-13 July, 2022*
*Bologna, Italy*

*on behalf of the LHCb collaboration





PoS(ICHEP2022)812

## 1. Introduction

Multi-body hadronic decays of charm particles offer an interesting environment for addressing a variety of phenomena related to the interplay of weak and strong interactions. Typically, the formation of three- and four-body final states proceeds through resonances as intermediate states (often assumed that the dynamics of the final states can be well represented as a quasi-two-body process, the "2+1" approximation [1], and are driven by meson-meson interactions). These resonances form rich interference patterns which allow the study of light meson spectroscopy, among other effects. This is particularly relevant for the controversial scalar sector, which poses a long-standing puzzle.

Previous analyses of the $D^+ \to \pi^-\pi^+\pi^+$ decays [1] [2–4] have shown a dominance of the S-wave component, with a $\sim$ 50% contribution from the $f_0(500)$ meson. The dominant decay mechanism is expected to be the tree-level external $W$-radiation amplitude, illustrated in Fig. 1, thus the $\pi^-\pi^+$ amplitudes, including the S-wave one, are produced primarily from a $d\bar{d}$ source. As a comparison, in the $D_s^+ \to \pi^-\pi^+\pi^+$ decay the S-wave contribution (produced via $s\bar{s}$) is also found to be dominant [5–7], but its main component is the $f_0(980)$ state, with no evidence for $f_0(500)$ production. At present, there is no complete description of the $\pi^-\pi^+$ S-wave amplitudes from first principles. In this proceedings report, two of the latest LHCb charm amplitude analysis are presented: $D^+ \to \pi^-\pi^+\pi^+$ [8] and $D_s^+ \to \pi^-\pi^+\pi^+$ [7] decays.

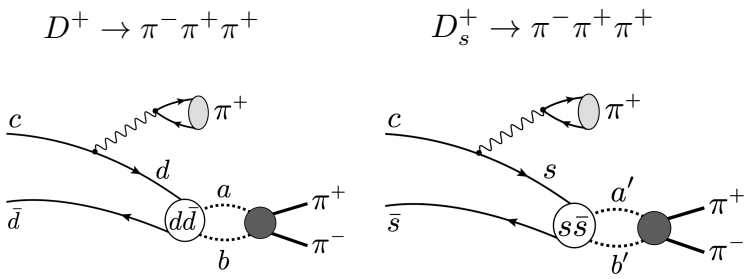


**Figure 1:** Leading order tree-level diagram for the $D^+ \to \pi^-\pi^+\pi^+$ and $D_s^+ \to \pi^-\pi^+\pi^+$ decays including a possible rescattering effect, represented by the $a, b$ meson pair.

## 2. The QMIPWA formalism

The Dalitz plot analysis of both decays is presented based on 1.5 fb$^{-1}$ of $pp$ collision data at 8 TeV centre-of-mass energy, collected by the LHCb experiment in 2012. The main purpose is to determine the resonant structure of the decay. The $\pi^-\pi^+$ S-wave is studied using a *quasi-model-independent* partial wave analysis (QMIPWA): no model is assumed for the S-wave amplitude, which is parameterised as a generic complex function to be determined by a fit to the data, while spin-1 and spin-2 states are included through an isobar model. The total amplitude is written as

$$\mathcal{A}\left(s_{12}, s_{13}\right) = \left[\mathcal{A}_{\text{S-wave}}(s_{12}) + \sum_i a_i e^{i\delta_i} \mathcal{A}_i\left(s_{12}, s_{13}\right)\right] + \left(s_{12} \leftrightarrow s_{13}\right), \tag{1}$$

[1] Charge conjugation is implicit unless otherwise stated.

where the total amplitude is Bose-symmetrised with respect to $s_{12}$ and $s_{13}$ due to the two identical pions. The first term is the S-wave amplitude,

$$\mathcal{A}_{\text{S-wave}}(s_{12}) = a_0(s_{12})e^{i\,\delta_0(s_{12})}, \tag{2}$$

where the real functions $a_0(s_{12})$ and $\delta_0(s_{12})$ are to be determined by the Dalitz plot fit: the $\pi^-\pi^+$ invariant-mass spectrum is divided in intervals (knots) where interpolation to obtain a continuous S-wave complex function is attained through a linear spline. The P- and D-wave components are included through an isobar model, represented by the terms in the sum in Eq. 1, where $\mathcal{A}_i\ (s_{12}, s_{13})$ is the complex amplitude of resonance $R_i$, with magnitude $a_i$ and phase $\delta_i$ as free parameters. This approach to the total amplitude is referred to as *quasi-model-independent* since any limitation of the isobar model to describe the higher-spin components may reflect in the description of the S-wave amplitude.

The invariant mass fits of the $D^+_{(s)} \to \pi^-\pi^+\pi^+$ candidates are shown in Fig. 2 (left plots). Only events inside a $2\sigma$ window around the peak with 95% purity are used for the fits. The Dalitz plot of the selected candidates are also shown in Fig. 2 (right plots). A rich resonant structure is observed: for the $D^+$ mode contributions from the subchannels $\rho(770)^0\pi^+$ (with an evident interference with $\omega(782)\pi^+$ in the $D^+$ case while as a pure contribution in the $D^+_s$ case), $f_0(500)\pi^+$ for the $D^+$, $f_2'(1525)$ for the $D^+_s$, $f_0(980)\pi^+$ and possible high-mass vector and tensor states are seen. To disentangle these contributions, a full amplitude analysis is needed.

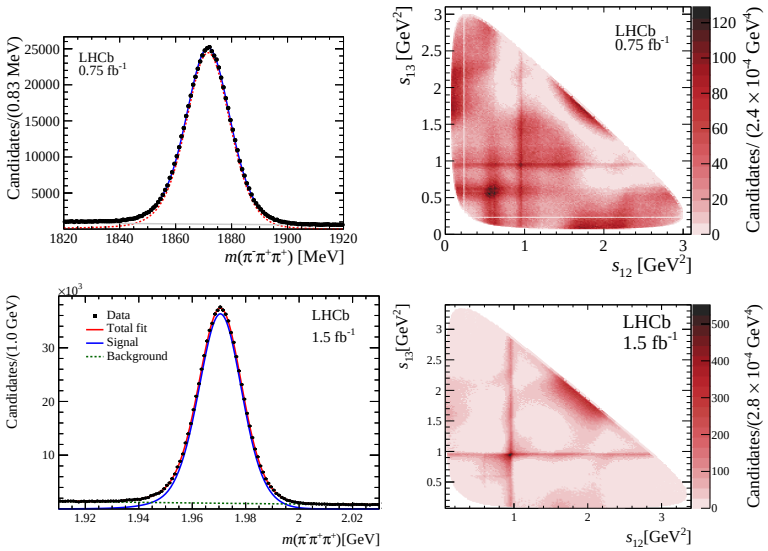


**Figure 2:** Invariant mass fit and Dalitz plot for the selected $D^+ \to \pi^-\pi^+\pi^+$ (top row) and $D^+_s \to \pi^-\pi^+\pi^+$ (bottom row) decays. The signal PDF is shown in red (blue) and the background in gray (green) for the $D^+$ ($D^+_s$) decay mode.

## 3. The Dalitz plot fit methodology

An unbinned maximum-likelihood fit to the data distribution in the Dalitz plot is performed. The likelihood function is written as a combination of the signal and background PDFs given by

$$\mathcal{L} = \prod_i \left\{ f_{\rm sig} \times \mathcal{P}^i_{\rm sig}\left(s_{12}, s_{13}\right) + \left(1 - f_{\rm sig}\right) \times \mathcal{P}^i_{\rm bkg}\left(s_{12}, s_{13}\right) \right\}, \tag{3}$$

where $f_{\rm sig}$ is the signal fraction and the product runs over the candidates in the final data sample. The background PDF, $\mathcal{P}_{\rm bkg}(s_{12}, s_{13})$, is the normalised background model, and is provided as a smoothed histogram. The normalised signal PDF, $\mathcal{P}_{\rm sig}(s_{12}, s_{13})$, is given by

$$\mathcal{P}_{\rm sig}\left(s_{12}, s_{13}\right) = \frac{\epsilon\left(s_{12}, s_{13}\right) \left|\mathcal{A}\left(s_{12}, s_{13}\right)\right|^2}{\iint_{\rm DP} \epsilon\left(s_{12}, s_{13}\right) \left|\mathcal{A}\left(s_{12}, s_{13}\right)\right|^2 ds_{12} ds_{13}}, \tag{4}$$

where $\epsilon(s_{12}, s_{13})$ is the efficiency model function included as the smoothed histogram; the denominator is the integral of the numerator over the Dalitz plot (DP) to guarantee that $\mathcal{P}_{\rm sig}\left(s_{12}, s_{13}\right)$ is normalised at each iteration of the minimisation process. The fit parameters are pairs of magnitudes and phases of the S-wave amplitude, and the magnitudes and phases of the higher-spin components, except the reference mode which has the magnitude fixed to 1 and phase fixed to zero. The set of optimal parameters is determined by minimising the quantity $-2\log\mathcal{L}$ using the `MINUIT` [9] package.

## 4. Amplitude analysis results

For the fit model for the $D^+ \to \pi^-\pi^+\pi^+$ mode, the S-wave is included using 50 knots and the higher spin contribution are: $\rho(770)^0\pi^+$, $\rho(1450)^0\pi^+$, $f_2(1270)\pi^+$, $\rho(1700)^0\pi^+$ plus the $\omega(782)\pi^+$ channel. From that, other possible states, such as $f_2'(1525)$, $\rho(1700)^0$, $\rho_3(1690)$, are added one at a time until a good representation of the data is found. For the $D_s^+ \to \pi^-\pi^+\pi^+$ mode, 50 knots are used plus the contributions: $\rho(770)^0\pi^+$, $\rho(1450)^0\pi^+$, $f_2(1270)\pi^+$, $\rho(1700)^0\pi^+$, $f_2'(1525)\pi^+$, and the $\omega(782)\pi^+$ channel. The projections and the fit results are shown in Figs. 3 and 4, showing overall a good agreement between the data and fit model.

## 5. $D^+ \to \pi^-\pi^+\pi^+$ vs $D_s^+ \to \pi^-\pi^+\pi^+$

The differences between the $\pi^+\pi^-$ S-wave amplitudes in $D_s^+ \to \pi^-\pi^+\pi^+$ and $D^+ \to \pi^-\pi^+\pi^+$ decays may be understood in the framework of the unitary chiral model [10]. The production of a pair of pseudoscalar mesons with zero orbital angular momentum could be energetically favoured compared to a scalar particle, *e.g.* quarks with spins aligned in an $L = 1$ state. The scalar mesons would be produced by the rescattering of the pair of pseudoscalar particles $ab \to \pi^+\pi^-$ $(a, b = \pi, K, \eta)$. The $d\bar{d}$ and $s\bar{s}$ pairs combine with $q\bar{q}$ pairs from the vacuum $(q = u,\ d,\ s)$, giving rise to different sets of pseudoscalar mesons and, therefore, to different S-wave amplitudes.

Considering the three possible light-quark pairs from the vacuum inserted between the $d\bar{d}$ pair, the $D^+$ decay has

$$d(\bar{u}u + \bar{d}d + \bar{s}s)\bar{d} = d\bar{u}u\bar{d} + d\bar{d}d\bar{d} + d\bar{s}s\bar{d}\,, \tag{5}$$

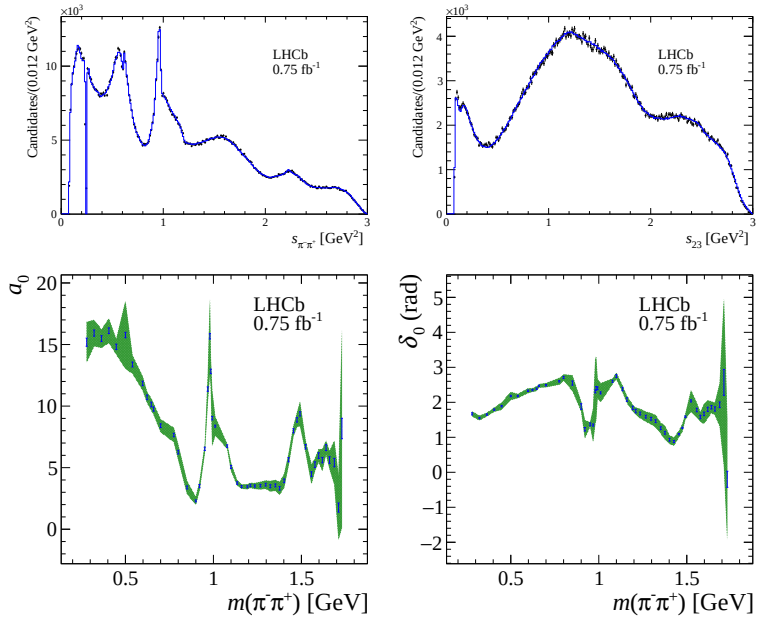


**Figure 3:** (top) Dalitz plot projections of $s_{\pi^-\pi^+}$ and $s_{23}$, where the (blue) line is the fit model result; (bottom) the fitted magnitude and phase of the $s_{\pi^-\pi^+}$ S-wave amplitude with statistical uncertainties as the blue bars and the total uncertainties (combined statistical, experimental and model systematics) as the green bands.

which, in terms of the pseudoscalar mesons, corresponds to

$$\sum_i d\bar{q}_i q_i \bar{d} = \pi^+\pi^- + \frac{1}{2}\pi^0\pi^0 - \frac{2}{\sqrt{6}}\pi^0\eta + K^0\bar{K}^0 + \frac{1}{3}\eta\eta \,. \tag{6}$$

In the $D^+ \to \pi^-\pi^+\pi^+$ decay, the S-wave would be formed by the reactions $ab \to \pi^+\pi^-$, with $ab = \pi^+\pi^-, \pi^0\pi^0, \pi^0\eta, K^0\bar{K}^0$ and $\eta\eta$. In the $D_s^+ \to \pi^-\pi^+\pi^+$ decay, $s(\bar{u}u + \bar{d}d + \bar{s}s)\bar{s}$ corresponds to

$$\sum_i s\bar{q}_i q_i \bar{s} = K^+K^- + K^0\bar{K}^0 + \frac{1}{3}\eta\eta \,, \tag{7}$$

leading to a different set of reactions $a'b' \to \pi^-\pi^+$, and therefore to different S-wave amplitudes. In this picture, the lack of an $f_0(500)$ contribution in the $D_s^+$ decay supports to the interpretation of this resonance as a dynamical pole of the $\pi\pi$ scattering. The $f_0(980)$ resonance is known to couple strongly to $K\bar{K}$, which can explain the relative prominence of this state in $D_s^+$ decays with respect to $D^+$ decays.

On the P-wave, the same resonances appear in both channels but with different contributions. The $\omega^0(782)\pi^+$ is observed for the first time in both channels, however, different production mechanisms are involved. The $\rho^0(770)$ is also present in both modes but contributing with different fit fractions. Furthermore, both $\rho^0(1450)$ and $\rho^0(1700)$ states are necessary for a good fit. On the D-wave, both modes have the $f_2(1270)$ as the largest contribution and only for the $D_s^+$ mode, the $f_2'(1525)$ is observed for the first time. From the results obtained from the amplitude analyses, one can conclude that even thought the two decay modes have the same final state, the resonant structure is very different. In particular, in the S-wave amplitude, the scalar resonances are produced via different mechanisms.

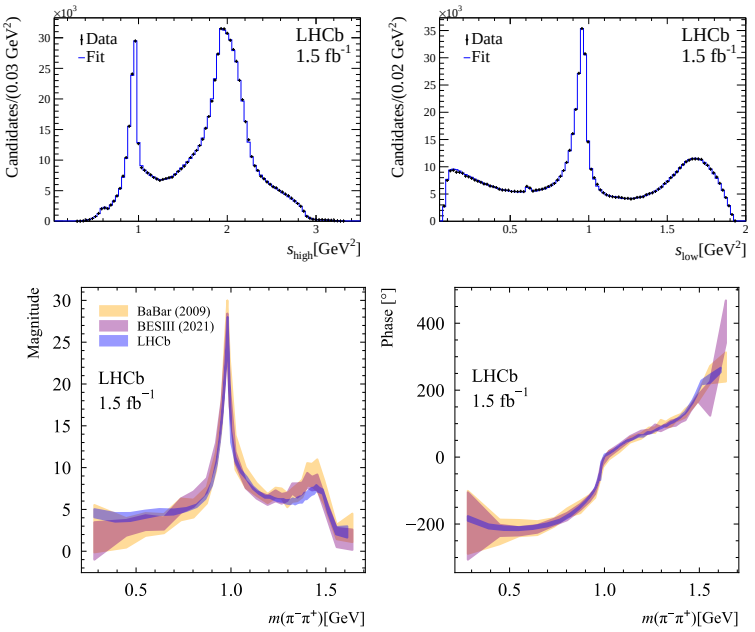


**Figure 4:** (top) $D_s^+ \to \pi^-\pi^+\pi^+$ Dalitz plot projections of $s_{high}$ and $s_{low}$, projections and (bottom) fitted magnitude and phase of the $\pi^-\pi^+$ S-wave amplitude with combined statistical, experimental and model systematic uncertainties compared to previous results from BaBar [5] and BESIII [6].

## References


[1] I. Bediaga and C. Göbel, *Direct CP violation in beauty and charm hadron decays*, *Prog. Part. Nucl. Phys.* **114** (2020) 103808 [2009.07037].

[2] E791 collaboration collaboration, *Experimental evidence for a light and broad scalar resonance in $D^+ \to \pi^-\pi^+\pi^+$ decay*, *Phys. Rev. Lett* **86** (2001) 770.

[3] FOCUS collaboration collaboration, *Dalitz plot analysis of $D_s^+$ and $D^+$ decay to $\pi^+\pi^-\pi^+$ using the K-matrix formalism*, *Phys.Lett.* **B585** (2004) 200.

[4] CLEO collaboration collaboration, *Dalitz plot analisis of the $D^+ \to \pi^-\pi^+\pi^+$ decay*, *Phys. Rev.* **D76** (2007) 012001.

[5] BaBar collaboration, *Dalitz Plot Analysis of $D_s^+ \to \pi^+\pi^-\pi^+$*, *Phys. Rev.* **D79** (2009) 032003 [0808.0971].

[6] BESIII collaboration, *Amplitude analysis of the $D_s^+ \to \pi^+\pi^-\pi^+$ decay*, 2108.10050.

[7] LHCb collaboration, *Amplitude analysis of the $D_s^+ \to \pi^-\pi^+\pi^+$ decay*, 2209.09840.

[8] LHCb collaboration, *Amplitude analysis of the $D^+ \to \pi^-\pi^+\pi^+$ decay and measurement of the $\pi^-\pi^+$ S-wave amplitude*, 2208.03300.

[9] F. James, *MINUIT function minimization and error analysis: Reference manual version 94.1*, 1994.

[10] E. Oset et al., *Weak decays of heavy hadrons into dynamically generated resonances*, *Int. J. Mod. Phys.* **25** (2016) 1630001.